A NUMERICAL INVESTIGATION ON THE EFFECT OF SMALL AND FLEXIBLE SEAGRASS *ZOSTERA NOLTII* ON WATER FLOW

Florian Ganthy[1], Romaric Verney[2], Aldo Sottolichio[3]

Abstract

The aim of this study was to provide a robust plant-flow interactions model to simulate impacts of *Zostera noltii* beds on hydrodynamics at different scales. To achieve this objective, the three-dimensional hydrodynamic model MARS-3D was implemented in order to take account for these small and flexible seagrass on currents. The effect of vegetation on hydrodynamics was introduced through the impact of cylindrical structures leading to additional source terms on drag and turbulent production and dissipation using the *k*-ε turbulence closure model. We introduced the seagrass flexibility throughout variables describing the vegetation: (1) the modification canopy height, (2) the modification of the diameter of plant structure induced by changing the angle between the leaf and the bottom and, (3) the modification of the vertical distribution of plant elements related to the modified canopy height. Three-dimensional formulations were then depth-averaged in order to decrease the computation time and investigate effects of model simplification on it accuracy. A two dimensional vertical (2DV) flume-like domain was defined to reproduce hydrodynamic conditions of flume experiments used for the model calibration. The 3D model was calibrated against velocity profiles sampled during these flume experiments. A good agreement between simulated and measured velocity profiles was obtained for different development stages of vegetation, both for the intensity and the shape of profiles with a total RMSE of 0.037 $m.s^{-1}$ over the 80 velocity profiles recorded. The flow establishment along a patch of finite vegetation was also well reproduced, denoting the suitability of the 3D model to simulate small-scale hydrodynamic processes induced by the vegetation on flow. The model was then applied to investigate impacts of seagrass characteristics on flow routing and bottom shear stress for two types of vegetation: flexible vegetation (*Z. notlii*) and an example of rigid vegetation like *Spartina* species. Results demonstrate that in both cases, near-bed velocities were significantly attenuated. This velocity attenuation was more efficient for flexible seagrass *Z. noltii* than for rigid vegetation such as *Spartina* species. These differences in velocity attenuation were attributed on one hand to the differences of the ratio between canopy height and water depth, driving the relative contribution between vertical and lateral flow deflexion, and one the other hand, by differences in vegetation densities controlling the loss of momentum due to wake-induced turbulence. Finally, the comparison of depth-averaged flow patterns between the 3D model and the 2DH model shown the limitation of the 2DH approach to simulate the fine-scale flow pattern and related bottom shear stress around vegetation patches (few metres), due to the non-taking account for vertical processes. However, the 2DH model suitability appears sufficient enough to be used at regional scale for long-term simulations of the impact of vegetation on morphological evolutions of coastal embayment due to its efficiency in terms of computation time (2-3 less expensive than the 3D approach).

Key words: seagrass, plant-flow interactions, bottom shear stress, 3D numerical modelling, *k*-ε turbulence closure scheme, *Zostera noltii*

1. Introduction

Seagrasses develop extensive underwater meadows in coastal areas around the world. Seagrass beds are in strong interaction with physical forcing, as they are affected by the flow, but they also modify hydrodynamics inside and around them (Gacia et al., 1999; Madsen et al., 2001). By damping hydrodynamic energy from tidal currents (Fonseca and Fisher, 1986; Gambi et al., 1990; Widdows et al.,

[1] University of Bordeaux, UMR EPOC, Avenue des Facultés, Talence 33405, France and IFREMER Centre de Brest, BP 70, Plouzané 29280, France. Now at the National Laboratory for Civil Engineering, Av. do Brasil 101, 1700-066, Lisboa, Portugal. fganthy@lnec.pt

[2]IFREMER Centre de Brest, BP 70, Plouzané 29280, France. rverney@ifremer.fr

[3]University of Bordeaux, UMR EPOC, Avenue des Facultés, Talence 33405, France. a.sottolichio@epoc.u-bordeaux1.fr

2008) and waves (Koch, 1999; Koch and Gust, 1999; Paul and Amos, 2011), seagrass canopies can strongly affect the transport of sediments and related erosion-deposition processes (Ward et al., 1984; Bouma et al., 2007; van Katwijk et al., 2010; Ganthy et al., 2011). Their presence in coastal shallow water may also impact the morphodynamic of coastal systems they colonized through significant seasonal and long-term modifications (Ganthy et al., 2013).
The Atlantic mesotidal lagoon of Arcachon presents wide intertidal areas extensively colonized by perennial seagrass meadows of *Zostera noltii*. Comparison of maps made in 1989 and 2007 showed that the surface area of these meadows has decreased by 33% from 68.5 km² to 45.7 km² (Plus et al., 2010). This decline has consequences not only for the ecology of the lagoon, but also for its management. At the same time as the meadow reduction in area, the inner channels are tending to fill in, increasing the need for dredging operations. Hence, numerical morphodynamic modelling integrating effects of seagrass *Zostera noltii* on flow and sediment dynamics is necessary to improve our understanding of the presence of seagrass beds and their decline on sedimentation and related morphological evolutions of the Arcachon lagoon, leading to better management decisions.
Over the last decade, numerous studies dealt with water flow modelling in presence of vegetation (Schutten and Davy, 2000; Verduin and Backaus, 2000; Abdelrhman, 2003; Erduran and Kutija, 2003; Uittenbogaard, 2003; Temmerman et al., 2005; Bouma et al., 2007; Casamitjana et al., 2012; Temmerman et al., 2012). Schutten and Davy (2000) predicted the hydraulic drag force of various kinds of vegetation throughout regression analysis from laboratory experiments. However their method did not provide information about the flow structure within the vegetation canopy. Abdelrhman (2003) achieved a good agreement with measured velocity profiles, after calibrating a substantial set of parameters, through the combination of formulations for above-canopy and within-canopy velocity profiles by matching the velocity at the top of canopy. From this strategy, the velocity profile will be continuous, but not the mass flux because of the discontinuity of the porosity at the top of the canopy (Nepf et al., 2007). Uittenbogaard (2003) simulated turbulent flows within and above rigid vegetation by introducing the competition between turbulence production and dissipation using the k-ε turbulence closure model (Rodi, 1980). His 1DV-model was extensively validated against flume experiments, and implemented within the 3D model DELFT3D. Its application dealt with the impact of vegetation on flow and sediment patterns in a tidal marsh/creek system (Temmerman et al., 2005, 2012) and to investigate the spatial flow and sedimentation patterns within and around patches of epibenthic structures (Bouma et al., 2007). This model allowed the good simulation of flow through rigid vegetation, but it did not take into account for leaf bending resulting from interactions between the water flow and flexible vegetation. In some previous studies, the vegetation bending and related canopy reconfiguration was taken into account throughout fully-physical formulations accounting for interactions between the ambient flow, the drag forces acting on separated leaves and, the leaf flexibility and buoyancy (Erduran and Kutija, 2003; Abdelrhman, 2007; Wilson, 2007). However, these physical formulations are time-consuming and require the knowledge of physical parameters (module of elasticity, buoyancy) which may vary in space and time depending on the seasonal seagrass development.

In this context, the aim of this study was to provide a robust plant-flow interaction model in order to simulate the impact of the small and flexible seagrass *Zostera noltii* on hydrodynamics from the scale of a laboratory flume (i.e. 1-10 m - to better understand small-scale processes) to the scale of coastal systems (i.e. 10^2-10^4 m – to investigate the effect of the presence of vegetation on sediment dynamics and associated morphological evolutions of such systems). To achieve this objective, the flow-vegetation model described by Uittenbogaard (2003) for rigid vegetation was integrated into the three-dimensional model MARS-3D (Lazure and Dumas, 2008). Then the seagrass flexibility was introduced throughout a semi-empirical method and the model was calibrated with flume experiments performed by Ganthy (2011). Afterward, the model was applied to investigate the impact of small and flexible seagrass *Zostera noltii* patches on flow and bottom shear stress, and to compare these effects with the effects of rigid vegetation such as *Spartina* spp. Finally, in a perspective of a long-term morphodynamic modelling, we also investigated the impact of model simplification (i.e. depth-averaged formulations) on it reliability to simulate vegetation-flow interactions.

2. Flume Experiments for Model Calibration

Flume experiments conducted by Ganthy (2011) were used for the model calibration. These experiments were performed within the HYDROBIOS flume (Orvain et al., 2003). The seagrasses *Zostera noltii* and their sediment clods came from a natural tidal flat of the Arcachon lagoon. They were collected and immediately placed into the flume forming a patch 0.9 m long and 0.4 m wide, under a water depth of 0.2 m. Four flow regimes were applied (from 0.08 to 0.38 $m.s^{-1}$, by steps of 0.1 $m.s^{-1}$). At each velocity regime, ADV velocity and turbulence profiles were measured at four longitudinal locations: 0.15 m upstream the seagrass patch, and 0.15, 0.45 and 0.75 m inside the vegetation patch. In the meantime, canopy height for each flow regime was determined from snapshots following a method derived from Neumeier (2005). After each test, a biometric analysis was performed following a protocol designed for the European Water Framework Directive (Auby et al., 2010a, 2010b). This analysis allowed the determination of the shoot density (D_{shoot}, in m^{-2}), the leaf length (L_l, in m), the number of leaf per shoot (N_l, dimensionless), the leaf width (w_l, in m) the leaf area index (*LAI*, total leaf area per ground area, dimensionless), and the vertical distribution of seagrass density (*n(z)*, dimensionless). A total of five experiments (Test T1 to T5) were performed between March and September 2010 to investigate effects of seagrass growth on hydrodynamics. A reference experiment was also performed on bare mud. A synthesis of seagrass characteristics obtained from these experiments and used for the model calibration is provided in Table 1.

Table 1. A synthesis of seagrass characteristics obtained during flume experiments (Ganthy, 2011) and used for the model calibration.

Parameter	Flume tests				
	T1	T2	T3	T4	T5
D_{shoot} ($\times 10^3$ m^{-1})	7.96	9.53	8.22	12.58	18.97
L_l (m)	0.056	0.072	0.066	0.063	0.151
N_l (-)	3.37	3.61	5.17	6.38	2.89
w_l (m)	0.00056	0.00058	0.00063	0.00082	0.0012
LAI (~)	0.85	1.42	1.78	4.22	9.03

3. Model Description

For this study we introduced the flow-vegetation interactions within the 3 dimensional hydrodynamic model MARS-3D (Model for Application at Regional Scale), developed by IFREMER (French Institute for Research and Exploitation of the Sea) for local to regional applications (Lazure and Dumas, 2008). The flow module computes flow characteristics (sea surface elevation, three-dimensional velocity components, and turbulence characteristics) over a three-dimensional grid using a finite difference solution. The MARS-3D model includes several eddy-viscosity based turbulence closure schemes, but for the purpose of this study the *k*-ε turbulence closure scheme (Launder and Spaling, 1974) was used. The bottom friction is modelled through a user specified roughness length (z_0). For further information about the MARS-3D hydrodynamic module, see Lazure and Dumas (2008).

3.1. *Three dimensional flow-vegetation model*

3.1.1. *General case: rigid vegetation*

The effect of rigid vegetation on hydrodynamics was implemented into the flow module through the impact of cylindrical vertical structures on drag and turbulence (Uittenbogard, 2003; Khublaryan, 2004; Casamitjana et al., 2012).

The influence of the cylindrical structures on drag leads to an additional source term in the momentum equations. The vertically distributed resistance forces imposed by the vegetation on the mean flow ($F_{veg}(z)$, in $N.m^{-3}$) is expressed as:

$$F_{veg}(z) = \frac{1}{2} \cdot c_D \cdot \rho_0 \cdot \phi(z) \cdot n(z) \cdot u(z) \cdot |u(z)| \quad (1)$$

Where c_D is the drag coefficient for vegetation, ρ_0 is the fluid density (in kg.m^{-3}), $\phi(z)$ is the diameter of cylindrical plant structure (in m) at the height z above the bed (in m), $n(z)$ is the number of plant elements per unit area (m^{-2}) at height z, and $u(z)$ is the horizontal flow velocity (m.s^{-1}) at height z above the bed.

The influence of the plant structures on turbulence leads to additional source terms in the turbulent kinetic energy, k (m^2.s^{-2}) and turbulent energy dissipation, ε (m^2.s^{-2}) formulations:

$$\left(\frac{\partial k}{\partial t}\right)_{veg} = \frac{1}{1 - A_{veg}(z)} \cdot \frac{\partial}{\partial z}\left\{\left(1 - A_{veg}(z)\right) \cdot \frac{(\upsilon + \upsilon_T)}{\sigma_k} \cdot \frac{\partial k}{\partial z}\right\} + T_{veg}(z) \quad (2)$$

$$\left(\frac{\partial \varepsilon}{\partial t}\right)_{veg} = \frac{1}{1 - A_{veg}(z)} \cdot \frac{\partial}{\partial z}\left\{\left(1 - A_{veg}(z)\right) \cdot \frac{(\upsilon + \upsilon_T)}{\sigma_\varepsilon} \cdot \frac{\partial \varepsilon}{\partial z}\right\} + T_{veg}(z) \cdot \tau_\varepsilon^{-1} \quad (3)$$

$$A_{veg} = \left(\frac{\pi}{4}\right) \cdot \phi^2(z) \cdot n(z) \quad (4)$$

Where $A_{veg}(z)$ is the horizontal cross-sectional plant area per unit area at height z (4), ν is the molecular fluid viscosity (m².s^{-1}), ν_t is the eddy viscosity (m².s^{-1}), σ_k is the turbulent Prandtl-Schmit number for self mixing of free turbulence (σ_k=1), $T_{veg}(z)$ is the work spent by the fluid (m².s^{-3}) at height z ($T_{veg}(z) = F_{veg}(z)u(z)/\rho_0$), σ_ε the turbulent Prandtl-Schmidt number for mixing of small-scale vorticity (σ_ε = 1.3), and τ_ε is the minimum between the dissipation timescale of free turbulence, τ_{free} (5) and the dissipation timescale of eddies between the plants, τ_{veg} (6).

$$\tau_{free} = \frac{1}{c_{2\varepsilon}} \cdot \left(\frac{k}{\varepsilon}\right) \quad (5)$$

$$\tau_{free} = \frac{1}{c_{2\varepsilon} \cdot \sqrt{c_\mu}} \cdot \left(\frac{{L_{veg}}^2}{T}\right)^{1/3} \quad (6)$$

With coefficient c_{2s}=1.96, c_μ=0.09 and L_{veg} is the typical size of eddies limited by the smallest distance between the plant structures (7).

$$L_{veg} = c_{lz} \cdot \left\{\frac{1 - A_{veg}(z)}{n(z)}\right\}^{1/2} \quad (7)$$

In (7), c_{lz} is a coefficient reducing the geometrical length scale to the typical volume averaged turbulence length scale, c_{lz} =0.3 was found applicable for vegetation (Uittenbogaard, 2003).

3.1.2. *Introduction of seagrass flexibility*

To take account for the seagrass flexibility, we choose a semi-empirical method in order to minimize model complexity and to save computational time. We introduced leaf bending within variables describing vegetation through: (1) the modification of canopy height, H_c, (2) the geometrical modification of the apparent diameter of plant structures, ϕ, induced by changing the angle between plant structure and the bottom (locally considered horizontal), (3) the modification of vertical plant distribution related to modified canopy height (i.e. the canopy reconfiguration), $n(z)$.

The deflected canopy height (H_c, in m) was computed at each time step using an empirical relationship (8) calibrated from flume experiments (Ganthy, 2011). This relationship integrates both the depth-averaged

current velocity from previous time-step (U, in cm.s^{-1}) and the dimensionless leaf area per unit of bed area (LAI).

$$H_c = a_h \times \frac{\left(a_0 + a_1 \cdot U + a_2 \cdot LAI + a_3 \cdot U \cdot LAI + a_4 \cdot U^2 + a_5 \cdot LAI^2\right)}{100} + b_h \quad (8)$$

Where a_0=4.647, a_1=-0.146, a_2=0.262, a_3=-0.011, a_4=0.002, and a_5=0.048 are coefficients for the polynomial relation to compute effective canopy height, while a_h=0.72 and b_h=-0.008 corresponds to the relation between effective canopy height and hydraulic canopy height (the level of the maximum of turbulent kinetic energy value).
The modification of the apparent plant element diameter by changing the angle (α) between the plant structures (i.e. leaves) and the bottom in the flow direction (ϕ_b), is taking account by introduction of a geometric correction associated with a calibration coefficient (c_w). In natural conditions for moderate to high velocities, leaves can reach the horizontal, leading to an apparent diameter in the flow direction tending to the leaf length (L_l). The coefficient c_w was introduced to artificially increase ϕ_a and to provide an estimation of this process. While the element diameter perpendicular to the flow direction (ϕ_b) remains equal to the leaf width (w_l).

$$\phi_a = c_w \cdot w_l \cdot \frac{H_c}{L_l} \quad (9)$$

$$\phi_b = w_l \quad (10)$$

In the formulation describing the force imposed by the vegetation onto the mean flow (1), we replaced ϕ by the mean value between ϕ_a and ϕ_b while for the cross-sectional plant area (A_{veg}, (4)), we consider an ellipse, leading to (11).

$$A_{veg} = \pi \cdot \left(\frac{\phi_a(z)}{2}\right) \cdot \left(\frac{\phi_b(z)}{2}\right) \cdot n(z) \quad (11)$$

Finally, as the vertical distribution of plant element changed when bending occurred, we used a realistic vertical distribution obtained from biometric data (Ganthy, 2011) normalized by the maximum number of elements (i.e. the product of the shoot density, D_{shoot} in m^{-2}, with the number of leaf per shoot, N_l, dimensionless) and, in the vertical direction z, by the leaf length (L_l, in m). The number of deflected plant element, n_d, was then defined as:

$$n_d = \sum_{z=H_c}^{z=L_l} n(z) \quad (12)$$

This number of deflected plant element, n_d, was then uniformly added to the original distribution between the bed ($z=0$) and the top of the canopy ($z=H_c$).

3.2. *Depth-averaged vegetation-flow model*

Modelling the impact of small vegetation compared with total water depth using three dimensional formulations may be very expensive in terms of computational time due to the requirement to define some vertical levels between the bed and the top of vegetation to be simulated. This requirement also leads to very short time-steps. In order to save computational time we also investigated the reliability of a depth-averaged integration of seagrass impacts on flow. To do this, we simply integrated over the depth the resistance forces imposed by vegetation on the mean flow within the two-dimensional momentum equation (1). While the roughness length, z_0, was set equal to the canopy height, H_c.

3.3. *Impact of vegetation on bottom shear stress*

For sediment dynamics modelling perspective, and because sediment erosion is assumed to be controlled by the bottom shear stress (τ_b), this parameters was also calibrated against results from flume experiments. In the general case of turbulent flows, τ_b is related to the velocity through a quadratic relationship (13).

$$\tau_b = \rho u^{*2} \tag{13}$$

Where the friction velocity, u^*, represents the intensity of turbulent velocity fluctuations within the bottom boundary layer. The friction velocity is generally computed assuming a logarithmic shape of the velocity profile within the bottom boundary layer (14).

$$u^* = \kappa \frac{u(z)}{\ln\left(z/Z_0\right)} \tag{14}$$

Within MARS-3D, the bottom shear stress is computed within the sediment module from a user-defined roughness length (Z_0) different from the roughness length used by the hydrodynamic module (z_0). This distinction between hydrodynamic and sediment roughness length (respectively z_0 and Z_0) allowed in the specific case of vegetation-flow interactions, to separate effects of vegetation on the vertical distribution of velocities from effects of vegetation on the bottom shear stress.

3.4. *Simulation settings*

3.4.1. *Model calibration*

A 2DV flume-like model domain (3.9 m length) was designed to reproduce hydrodynamic conditions observed during the flume experiments from Ganthy (2011). The horizontal resolution was set to 0.15 m, while forty logarithmically distributed vertical layers were defined in order to obtain the highest resolution near the bed and within the canopy (vertical resolutions ranges from 2.7 mm near the bed to 30 mm near the surface). The domain was forced at its western boundary (entrance of the flume) by a constant inflow corresponding to a chosen depth averaged velocity. Sea surface elevation was set free at the entrance of the flume and set to zero at the exit (eastern boundary), while constant depth (0.2 m) was defined along the domain. The vegetation patch was placed at 1.95 m from the flume entrance and extended over 1.05 m (0.15 m longer than for flume experiments, corresponding to one more computational cell).

The model calibration was performed through the adjustment of the drag coefficient, c_D, and the anisotropic leaf width coefficient, c_w, by running the model for every experimental test and every velocity treatment (sets of 20 simulations). The couple (c_D, c_w) providing the lowest root mean square error (RMSE) over each measured velocity profiles (4 locations * 4 velocities * 5 tests) was then retained. After hydrodynamic calibration of velocities, the roughness length for sediment transport, Z_0, was then calibrated following the same methodology, in order to obtain the best agreement between measured and simulated bottom shear stress.

3.4.2. *Investigations on characteristics of the vegetation and model simplifications*

A 3D flume-like domain (20 m length, 10 m wide) was designed to investigate the effects of seagrass flexibility and model simplifications (3D and 2DH) on flow routing and possible implications for sediment transport for a patchy distribution. The horizontal grid resolution was set to 0.15 m (x and y directions), while forty logarithmically distributed vertical layers were defined. A constant depth (0.4 m) was defined over the entire domain. As for model calibration, the domain was forced at the western boundary by a constant inflow corresponding to a depth averaged velocity of 0.3 $m.s^{-1}$. Ten circular vegetation patches (diameter = 2 m) were defined in staggered rows spatial organisation leading to minimum and maximum distance between patches equal to 1.4 and 3.5 m respectively.

Two simulations were performed (one using 3D and one using 2DH formulations) with high density of flexible seagrass *Z. noltii* (vegetation parameters from the test T5, Table 1). Also, one simulation with rigid vegetation like *Spartina* spp. was performed using 3D formulations. In the latter case, vegetation

parameters were derived from Bouma et al. (2007) and corresponds to canopy height (H_c) of 0.2 m, leaf width (w_l) of 0.008 m and the number of plant element ($n(z)$, constant) of 400 m^{-2}.

4. Results and Discussion

4.1. *Model reliability*

Using the 3D formulations, the best agreement between measured and simulated velocity profiles was found for c_D equal to 1.5 and c_w equal to 2.41, with a total RMSE of 0.037 $m.s^{-1}$ over all velocity profiles (all longitudinal position, all velocities and all tests). From the comparison of measured and simulated velocity profiles for tests presenting the lowest (test T1, Figure 1a) and the highest (test T5, Figure 1b) seagrass development, velocities appear better simulated for lower velocities. While for higher velocities, the velocity above the canopy was slightly underestimated for the low density test. However, in all cases, the shape of simulated velocity profiles was similar to the shape of measured velocity profiles. The scatter plots between measured and simulated velocities for the different positions along the vegetation patch (Figure 1c to 1f) and associated RMSE, shows that velocity profiles simulated at 0.15 m upstream the vegetation patch were the closest to measurements (RMSE = 0.21 $m.s^{-1}$). Considering velocities inside vegetation patch, better results are obtained for the profiles located at 0.45 m (RMSE = 0.027 $m.s^{-1}$) and 0.75 m from the upstream edge of the vegetation patch. While for the profile located at 0.15 m from the upstream edge, the lower agreement was obtained (RMSE = 0.053 $m.s^{-1}$), this position corresponding to the first computational cell inside the vegetation patch.

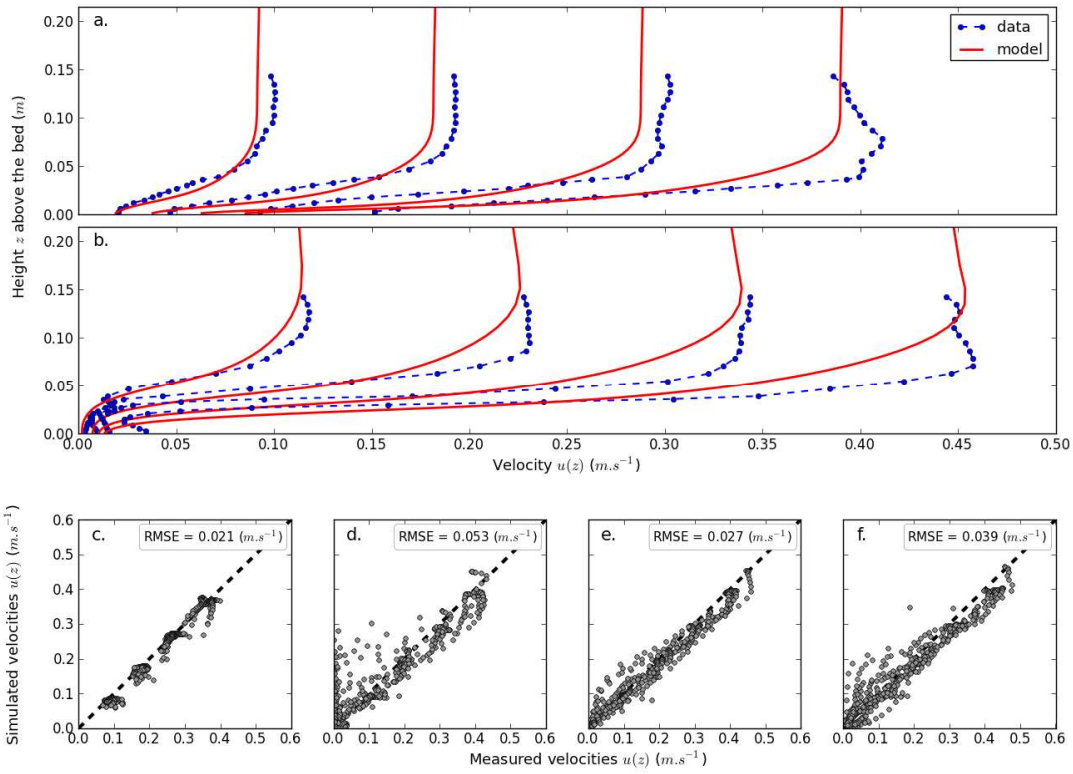

Figure 1. Upper panels: comparison between measured (blue dashed marked lines) and simulated (red line) velocity profiles at 0.45 m from the vegetation edge for the four velocity treatments for the lowest (test T1, a) and the highest (test T5, b) seagrass development. Lower panels: scatter plots between measured and simulated velocities (grey dots) presented with their associated root mean square errors (RMSE) at 0.15 m upstream (c), 0.15 m (d), 0.45 m (e) and 0.75 m (f) downstream the edge of vegetation patch. The unity line (black dashed line) is also provided.

When comparing our model results with other studies using similar mathematical formulations (Baptist,

2003; Uittenbogaard, 2003) our model may appear less accurate for predicting velocity profiles in vegetated flows. However, these authors used a 1DV model for their calibration. In this kind of model, the main assumption is that the flow is uniform in the horizontal direction. In other words, they assumed that vegetation extends infinitely in horizontal direction, which does not correspond to the reality from flume experiments used for the model calibration, where vegetation patch had a finite length (0.9 m).
Numerous studies have demonstrated a significant increase in flow reduction within the canopy with the distance from the leading edge of the vegetation patch (Fonseca and Fisher, 1986; Gambi et al., 1990; Fonseca and Koehl, 2006). We also verified the ability of our model to simulate this flow establishment along the vegetation patch. The Figure 2, showing the vertical distribution of velocities along the domain for a low vegetation development (Figure 2a to 2e) and a high vegetation development (Figure 2f to 2j) demonstrates the ability of the 3D model to simulate longitudinal modification of the vertical flow structure induced by the vegetation.

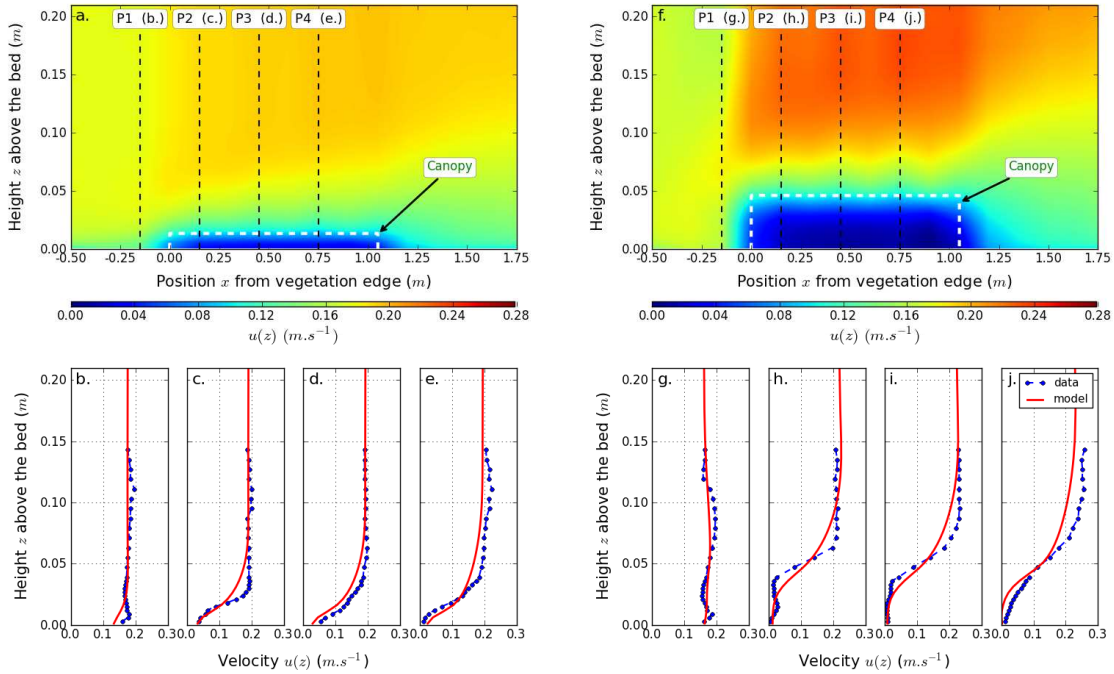

Figure 2. Distribution of velocities along the domain for the test T2 (low vegetation development, a) and test T5 (high vegetation development, f). Velocity profiles (black dashed lines) and vegetation localization and height (white dashed line) are also indicated. b, c, d and e, comparisons between simulated and measured velocity profiles taken at the four *x* positions relative to the vegetation edge (respectively at 0.15 m, 0.45 m and 0.75 m downstream the vegetation edge) for the test T2, and g, h, i and j for the test T5.

4.2. *Effects of vegetation characteristics*

We investigated the impact of vegetation characteristics by comparing spatial distribution of velocities averaged from the bed to the top of the canopy, from the top of canopy to the water surface, and the bottom shear stress for high *Z. noltii* density and high density of rigid vegetation like *Spartina* spp. (Figure 3). Considering velocities averaged from the top of canopy to the water surface (Figure 3a and 3b), the presence of vegetation patch leads to an increase of velocities over the canopy, for both types of vegetation simulated. This increase of velocity is however considerably stronger in presence of *Spartina*-like vegetation (increase of 0.02 $m.s^{-1}$ for *Z. noltii* and 0.1 $m.s^{-1}$ for *Spartina*) and associated to a flow divergence at the downstream part of *Spartina* patches. In the meantime, velocities averaged from the bed to the top of canopies shows a significant decrease for both types of vegetations (Figure 3c and 3d). However, for the case of *Z. noltii* (Figure 3c) velocities shows a slight increase located at the upstream edge of patches, followed by a drastic decrease along the first few centimetres inside patches. By contrast, for *Spartina*, velocities tends to decrease continuously from upstream to downstream edge of patches

(Figure 3d) and shows more pronounced wake-effect and lateral flow deflection than for *Z. noltii*. These differences of horizontal flow patterns between the two types of vegetations could be explained by two mechanisms. On one hand, the differences in the ratio between the canopy height and the water depth which is well known to strongly impact the relative importance between the vertical and lateral flow deflection (Fonseca and Koehl, 2006; Nepf et al., 2007). For *Z. noltii* the canopy occupy less than 1/10 of the total water depth, while for *Spartina* spp. canopy occupy 1/2 of the water depth. Also, despite less density and velocity attenuation, the lateral flow deflection plays a major role in case of higher vegetation. One the other hand, vegetation density has strong effects on momentum loss related to wake-induced turbulence (Nepf, 1999). These effects are not only induced by the absolute vegetation density, but also by the impact of vegetation flexibility which lead to an increase of density near the bed at high velocity (i.e. canopy reconfiguration) in the case of Z. noltii.
Considering the bottom shear stress, τ_b, similar spatial pattern as for near-bed velocities are obtained for the case of *Z. noltii* (Figure 3e): a slight increase located at the upstream edge of patches, followed by a drastic decrease along the first few centimetres inside patches. While, for Spartina (Figure 3f) the bottom shear stress increases significantly (from 0.7 to 2.3 N.m-*2*) within the upstream parts of vegetation patches and afterward it tends to decreases along the patches to reach minimum levels downstream the end of patches. Similar spatial patterns of bottom shear stress for *Spartina*-like vegetation were also obtained by Bouma et al. (2007).

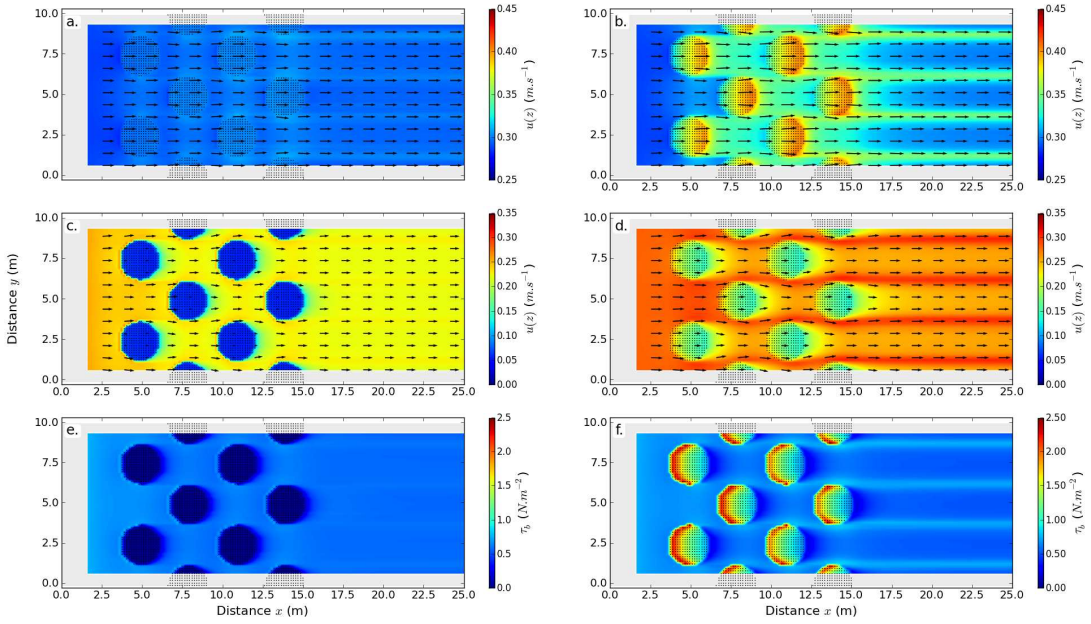

Figure 3. Horizontal distribution of velocities averaged above canopy (a and b), inside canopy (c and d), and bottom shear stress (e and f) simulated for flexible seagrass *Z. noltii* (a, c and e) at high density (test T5) and for rigid vegetation like *Spartina* spp. (b, d and e) at high density (3D model). Note that differences in near-bed velocities from *Z. noltii* (c) and *Spartina* spp. (e) are induced by the differences in vegetation height over which velocities are integrated.

Finally, considering the bottom shear stress as a proxy of sediment resuspension, the seagrass *Zostera noltii* appears to be more efficient to protect bed sediments from erosion than other rigid species like *Spartina* spp., due to their flexibility and small size compared to the water depth.

4.3. *Impacts of model simplifications on flow*

Comparisons between depth-averaged velocities simulation for high density of *Z. noltii* using the 3D model (Figure 4a) and the 2DH model (Figure 4b) show significant differences in flow patterns. Depth-averaged velocities simulated using the 3D model are quite homogeneous, both in terms of magnitude and direction. Velocities are weakly attenuated within vegetation patches (0.22 m.s^{-1}) compared with velocities around

patches (0.26 m.s^{-1}). By contrast, using the 2DH model, simulated velocities show important spatial heterogeneity, with significantly lower velocities inside vegetation patches (less than 0.2 m.s^{-1}) and important acceleration around them (up to 0.3 m.s^{-1}), associated with important wake-effects downstream patches. These differences of horizontal depth-averaged flow patterns between the 3D model and the 2DH model are directly related to the differences in hydrodynamic processes taken into account. Using the 3D model, the flow appears mostly redirected above the canopy (i.e. vertical deflexion of flow), except near the patch sides where horizontal deflection may be significant (Figure 3a to 3d, more important for rigid species). The velocity enhancement above the vegetation patch also predominates over velocity increase around the patches, so that depth-averaged velocities look quite homogeneous. While using the 2DH model, the vertical flow deflexion is not taken into account, so that the totality of the flow is laterally deflected, leading to important velocity enhancement around vegetation patches.
Differences in horizontal flow structures depending on model formulations may also imply important effects on sediment transport, as shown in Figure 4c and 4e, through the differences in the bottom shear stress levels (used as a proxy of sediment resuspension). However, as the ratio between the canopy height and the water depth impacts the relative importance between the vertical and lateral flow deflexion (Fonseca and Koehl, 2006; Nepf et al., 2007) the differences of flow velocities and sediment transport between the two model formulations will be related to it. In case of emergent vegetation, the vertical flow deflexion is nearly inexistent, leading to the reduction of the errors of the 2DH model. Moreover, important canopy height/water depth ratio (i.e. very small vegetation compared to water depth) will also tend to reduce errors associated to the 2DH model, throughout the weaker impacts of vegetation canopy compared to the mean ambient flow.

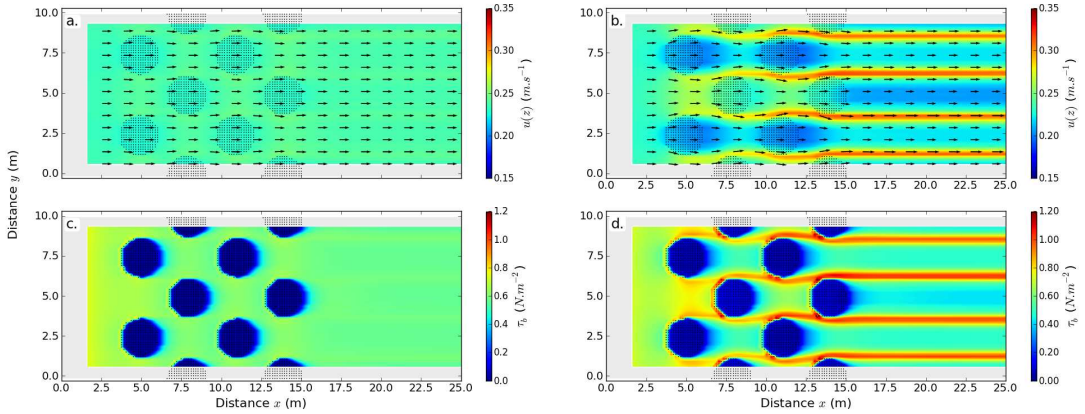

Figure 4. Horizontal distribution of depth-averaged velocities (a and b) and bottom shear stress (c and d) simulated for flexible seagrass *Z.noltii* at high density (test T5) using the 3D formulations (a and c) and the 2DH formulations.

Finally, despite a less accuracy of the 2DH model compared with the 3D model to simulate small-scale effects, the 2DH model is 2-3 fold less expensive in computational time and appears suitable enough to be used at the scale of a coastal system to simulate long-term morphological evolutions of coastal areas in presence of benthic vegetation.

5. Conclusion

The introduction within the MARS-3D model of the balance between turbulence production and dissipation, associated with a semi-empirical method for taking account for seagrass flexibility allowed to simulate a wide range of 3 dimensional flows through both rigid and flexible vegetation. A good agreement between simulated and measured velocity profiles was obtained for different development stages of the seagrass *Zostera noltii*, both for the shape of the velocity profiles and intensity. The longitudinal flow pattern along a finite patch of seagrass was also well reproduced, denoting the ability and suitability of the model to simulate small-scale hydrodynamic processes induced by the vegetation on flow. The investigations performed over the impact of vegetation characteristics demonstrated that the 3D model will offer a robust and valuable tool to further insight in understanding small-scale flow-vegetation processes,

such as impacts of the ratio between canopy height and the water depth on the relative contribution between vertical and lateral flow deflection above and around vegetation patches and on the spatial pattern of sediment transport at the patch scale. The 3D model appears also suitable to simulate these plant-flow interactions and their implications for sediment dynamics at larger scales, such as the regional scale of the Arcachon lagoon. However, short time steps induced by the important near-bed vertical discretization led us to investigate the reliability of a 2DH approach to simulate vegetation-flow interactions effects on sediment transport and resulting morphological evolutions of coastal systems. The comparison of small-scale (few metres) horizontal flow patterns and associated bottom shear stress between the 3D and the 2DH approach highlighted the limitations of the 2DH approach to well simulate edge effects around a patch of vegetation. However, despite its less reliability than the 3D approach, the 2DH model could be considered to be relevant enough to be applied to simulate the impact of vegetation on flow and related morphological evolutions of the Arcachon lagoon. Indeed, errors are expected to be reduced at larger spatial scales, and efficiency is gained in terms of computational time.

Acknowledgements

This work is supported by IFREMER (French Inst. for Research and Exploitation of the Sea), SIBA (Syndicat Intercommunal du Bassin d'Arcachon), the Aquitaine Regional Council, INSU-CNRS and the University of Bordeaux 1, and was a part of the french research project EC2CO-EMPHASE. Sincere acknowledgements are given to Franck Dumas and Pascal Lazure (IFREMER) for their precious assistance with the open boundary management and the numerical scheme of the turbulence closure model within the MARS-3D code.

References

Abdelrhman, M.A., 2003. Effect of eelgrass *Zostera marina* canopies on flow and transport. *Marine Ecology Progress Series*, 248: 67-83.

Auby, I., Oger-Jeanneret, H., Sauriau, P.-G., Hily, C., and Barillé, L., 2010a. Angiospermes des côtes françaises Manche-Atlantique. Proposition pour un indicateur DCE et première estimation de la qualité. *IFREMER report*, p. 72.

Auby, I., Oger-Jeanneret, H., Sauriau, P.-G., Hily, C., and Barillé, L., 2010b. Angiospermes des côtes françaises Manche-Atlantique. Propositions pour un indicateur DCE et premières estimations de la qualité. Annexe 2 : Fiches contenant les données sur les herbiers des différentes masses d'eau suivies dans le cadre de la DCE. *IFREMER report*, p. 152.

Baptist, M.J., 2003. A flume experiment on sediment transport with flexible, submerged vegetation. *International Workshop on Riparian Forest Vegetated Channels: Hydraulic, Morphological and Ecological Aspects, RIPFOR, Trento, Italy.*

Bouma, T.J., van Duren, L.A., Temmerman, S., Claverie, T., Blanco-Garcia, A., Ysebaert, T. and Herman, P.M.J., 2007. Spatial flow and sedimentation patterns within patches of epibenthic structures: Combining field, flume and modelling experiments. *Continental Shelf Research*, 27: 1020-1045.

Casamitjana, X., Pujol, D., Colomer, J., and Serra, T., 2012. Application of a *k*-ε formulation to model the effect of submerged aquatic vegetation on turbulence induced by an oscillating grid. *Continental Shelf Research*, 34:1-6.

Erduran, K.S. and Kutija, V., 2003. Quasi-three-dimensional numerical model for flow through flexible, rigid, submerged and non-submerged vegetation. *Journal of Hydroinformatics*, 05(3): 189-202.

Fonseca, M.S. and Fisher, J.S., 1986. A comparison of canopy friction and sediment movement between four species of seagrass with reference to their ecology and restoration. *Marine Ecology Progress Series*, 29: 15-22.

Fonseca, M.S. and Koehl, M.A.R., 2006. Flow in seagrass canopies: the influence of patch width. Estuarine, *Coastal and Shelf Science*, 67: 1-9.

Gacia, E., Granata, T.C. and Duarte, C.M., 1999. An approach to measurement of particle flux and sediment retention within seagrass (*Posidonia oceanica*) meadows. *Aquatic Botany*, 65: 255-268.

Gambi, M.C., Nowell, A.R.M. and Jumars, P.A., 1990. Flume observations on flow dynamics in *Zostera marina* (eelgrass) beds. *Marine Ecology Progress Series*, 61: 159-169.

Ganthy, F., 2011. Rôle des herbiers de zostères (*Zostera noltii*) sur la dynamique sédimentaire du Bassin d'Arcachon. *PhD thesis, Université Bordeaux 1*.

Ganthy, F., Sottolichio, A. and Verney, R., 2011. The stability of vegetated tidal flats in a coastal lagoon through quasi in-situ measurements of sediment erodibility. *Journal of Coastal Research*, SI 64:1500 - 1504.

Ganthy, F., Sottolichio, A. and Verney, R., 2013. Seasonal modification of tidal flat sediment dynamics by seagrass

meadows of Zostera noltii (Bassin d'Arcachon, France). *Journal of Marine Systems*, 109-110:S233-S240.

Granata, T.C., Serra, T., Colomer, J., Casamitjana, X., Duarte, C.M. and Gacia, E., 2001. Flow and particle distribution in a nearshore seagrass meadow before and after a storm. *Marine Ecology Progress Series*, 218: 95-106.

Khublaryan, M.G., Frolov, A.P. and Zyryanov, V.N., 2004. Modeling water flow in the presence of higher vegetation. *Water Ressources*, 31(6):617-622.

Koch, E.W., 1999. Sediment resuspension in a shallow *Thalassia testudinum* banks ex König bed. *Aquatic Botany*, 65: 269-280.

Koch, E.W. and Gust, G., 1999. Water flow in tide- and wave-dominated beds of the seagrass *Thalassia testudinum*. *Marine Ecology Progress Series*, 184: 63-72.

Launder, B.B. and Spalding, D.B., 1974. The numerical computation of turbulent flow. *Computer Methods in Applied Mechanics and Engineering*, 3(2): 269-289.

Lazure, P. and Dumas, F., 2008. An external-internal mode coupling for a 3D hydrodynamical model for application at regional scale (MARS). *Advances in Water Ressources*, 31: 233-250.

Madsen, J.D., Chambers, P.A., James, W.F., Koch, E.W. and Westlake, D.F., 2001. The interaction between water movement, sediment dynamics and submersed macrophytes. *Hydrobiologia*, 444: 71-84.

Nepf, H., 1999. Drag, turbulence, and diffusion in flow through emergent vegetation. *Water Ressources Research*, 35:479-489.

Nepf, H.M., White, B., Ligthbody, A. and Ghisalberti, M., 2007. Transport in aquatic canopies. In: Gayev Y.A. and Hunt J.C.R. (Editors), *Flow and Transport Processes with Complex Obstructions*.

Neumeier, U., 2005. Quantification of vertical density variations of salt-marsh vegetation. *Estuarine, Coastal and Shelf Science*, 63: 489-496.

Orvain, F., Le Hir, P. and Sauriau, P.-G., 2003. A model of fluff layer erosion and subsequent bed erosion in the presence of the bioturbator, *Hydrobia ulvae*. *Journal of Marine Research*, 61: 823-851.

Paul, M. and Amos, C.L., 2011. Spatial and seasonal variation in wave attenuation over *Zostera noltii*. *Journal of Geophysical Research*, 116:C08019.

Plus, M., Dalloyau, S., Trut, G., Auby, I., de Montaudouin, X., Emery, E., Noël, C. and Viala, C., 2010. Long-term evolution (1988-2008) of *Zostera* spp. meadows in Arcachon Bay (Bay of Biscay). *Estuarine, Coastal and Shelf Science*, 87: 357-366.

Rodi, W., 1980. Turbulence models and their applications in hydraulics: a state of the art review. *International Association for Hydraulic Research*, Delft, Netherlands.

Schutten, J. and Davy, A.J., 2000. Predicting the hydraulic force on submerged macrophytes from current velocity, biomass ans morphology. *Oecologia*, 123: 445-452.

Temmerman, S., Bouma, T.J., Govers, G., Wang, Z.B., De Vries, M.B. and Herman, P.M.J., 2005. Impact of vegetation on flow routing and sedimentation patterns: three-dimensional modeling for a tidal marsh. *Journal of Geophysical Research*, 110: F04019.

Temmerman, S., Moonen, P., Schoelynck, J., Govers, G., and Bouma, T.J., 2012. Impact of vegetation die-off on spatial flow patterns over a tidal marsh. *Geophysical Research Letters*, 39:L03406.

Uittenbogaard, R., 2003. Modelling turbulence in vegetated aquatic flows. *International Workshop on Riparian Forest Vegetated Channels: Hydraulic, Morphological and Ecological Aspects, RIPFOR, Trento, Italy*.

van Katwijk, M.M., Bos, A.R., Hermus, D.C.R. and Suykerbuyk, W., 2010. Sediment modification by seagrass beds: muddification and sandification induced by plant cover and environmental conditions. *Estuarine, Coastal and Shelf Science*, 89: 175-181.

Verduin, J.J. and Backhaus, J.O., 2000. Dynamics of plant-flow interactions for the seagrass *Amphibolis antartica*: field observations and model simulations. *Estuarine, Coastal and Shelf Science*, 50: 185-204.

Ward, L.G., Kemp, W.M. and Boynton, W.R., 1984. The influence of waves and seagrass communities on suspended particulates in estuarine embayment. *Marine Geology*, 59: 85-103.

Widdows, J., Pope, N.D., Brinsley, M.D., Asmus, H. and Asmus, R.M., 2008. Effects of seagrass beds (*Zostera noltii* and *Z. marina*) on near-bed hydrodynamics and sediment resuspension. *Marine Ecology Progress Series*, 358: 125-126.

Wilson, C.A.M.E., 2007. Flow resistance models for flexible submerged vegetation. *Journal of Hydrology*, 342: 213-222.